

Numerical Solvers for Radiation and Conduction in High Temperature Gas Flows *

Mohammed Seaïd, Axel Klar, René Pinnau

Fachbereich Mathematik, Technische Universität Darmstadt, D-64289 Darmstadt, Germany

Abstract. In this paper, the authors introduce a robust numerical technique for radiation-conduction heat transfer in the high-temperature fields of gas turbine combustors. The conduction and radiation effects are analyzed by a differential and an integral equation, respectively. Using discrete ordinates for the angular discretization of the integral equation for the radiation effects and a Galerkin discretization for the heat equation, the authors propose a fast multilevel algorithm to solve the fully discretized problem. The algorithm uses the same mesh hierarchy for both radiation and conduction effects, but with two different smoothing operators. Numerical results are shown for test problems in three space dimensions, and comparisons to other methods are also given.

Keywords: Radiation-conduction heat transfer, Discrete ordinates, Galerkin method, Multilevel algorithms

1. Introduction

Thermal radiation in gas flows can be an important mode of heat transfer in high temperature chambers, such as industrial furnaces and boilers, even under non-soot conditions. Growing concern with high temperature processes has emphasized the need for an evaluation of the effect of radiative heat transfer. Nevertheless, the modeling of radiative is often neglected in combustion analysis, mainly because it involves tedious mathematics, which increase the computation time, and also because of the lack of detailed information on the optical properties of the participating media and surfaces. Ignoring radiative transfer may introduce significant errors in the overall predictions, for more discussions we refer the reader to (Jamaluddin and Smith, 1988, Selcuk, 1988, Selcuk and Kayakol, 1997, Liu et al., 1998).

The most accurate procedures available for computing radiation transfer in furnaces are the Zonal (Jamaluddin and Smith, 1988) and Monte Carlo (Steward and Cannom, 1971) methods. However, these methods are not widely applied in comprehensive combustion calculations due to their large computational time and storage requirements. Also, the equations of the radiation transfer are in non-differential

* This work was supported by the German Research Foundation (DFG), SFB568.

form, a significant inconvenience when solved in conjunction with the differential equations of flow and combustion. For this reason, numerous investigations are currently being carried out worldwide to assess computationally efficient methods. This paper deals with the design of such methods and shows that multilevel algorithm provides advantages that should be utilized in treating radiative transfer problems with or without flow convection.

Much of the current work on modeling energy transport in high-temperature gas or chemically reacting flows, uses computational fluid dynamics (CFD) codes. Therefore, the models for solving the radiative transfer equations must be compatible with the numerical methods employed to solve the transport equations. The Zonal and Monte Carlo methods for solving the radiative transfer problem are incompatible with the mathematical formulations used in CFD codes, and require prohibitive computational times for spatial resolution desired. The discrete ordinates methods (Chandrasekhar, 1950, Fiveland, 1991) appear to be reasonable compromises for solving the radiative transfer equations.

It is well known from the analysis on partial differential equations that the convergence rate in iterative methods is a function of spatial frequencies. Particularly, the longest wavelengths exhibit the lowest convergence rate, while short scales converge faster. To improve convergence, acceleration techniques based on spatial coarsening have been proposed in the literature, see for instance (Briggs et al., 1999, McCormick, 1989, Hackbusch, 1985). In the present work, we develop a multilevel technique for the radiation-conduction problems. The basic idea of the multilevel technique is to treat the modes with low spatial frequencies on coarser grids, since fine spatial resolution is not required for these modes. The gain of the method is due to the faster convergence of the long-wave modes on the coarser grids, as well as the lower CPU cost of the corresponding iterations.

The main objective of this work is to develop robust and efficient solvers for the radiative heat conduction problems. For the radiative transfer step, the problem is written as a compact linear system for mean intensity, then the Atkinson-Brakhage is used as an approximate inverse of the iterate matrix at the coarse mesh. Whereas, using a fully implicit time integrator, the heat conduction step is written as a nonlinear fixed point problem in temperature only, and a multilevel algorithm using Newton-Gmres as coarse mesh smoother on the same mesh hierarchy as in the radiative transfer step, is considered.

The paper is organized as follows: in section 2, we recall mathematical equations for radiation-conduction used to formulate the fast multilevel algorithm. The formulation of the algorithm is given in section

3. We describe with some details the stages constituting the implementation of the algorithm namely: (i) time, space and ordinate discretizations, (ii) grid hierarchy, prolongation and projection operators, and (iii) the coarse mesh solvers. Section 6 is devoted to numerical results for two three-dimensional test examples. Finally, section 5 contains some concluding remarks.

2. Radiation-Conduction Equations

As mentioned in the introduction, in the present work we are mainly interested on developing efficient solvers only for the radiative heat conduction in gas flows. Thus, we assume a suitable set of equations is used for the hydrodynamics from which the velocity field is updated and consequently used for convection in the heat equation.

Given a convex spatial domain $\Omega \subset \mathbb{R}^3$ the radiation-conduction heat equations we consider in this paper consist of the heat conduction equation

$$\rho c \frac{\partial T}{\partial t} + \mathbf{u} \cdot \nabla T - \nabla \cdot (K \nabla T) = - \int_{\nu_0}^{\infty} \int_{\mathbb{S}^2} \kappa (B(T, \nu) - I) d\omega d\nu, \quad (1)$$

where ρ is the density, c denotes the specific heat capacity, T the temperature, K the thermal conductivity and \mathbf{u} is the flow velocity provided by a hydrodynamic model (for example Navier-Stokes equations). $I(\nu, \mathbf{x}, \omega)$ represents the spectral intensity for frequency ν at point \mathbf{x} traveling in direction $\omega \in \mathbb{S}^2$, where \mathbb{S}^2 is the unit sphere. The spectral intensity is obtained from the radiative transfer equation

$$\forall \nu > \nu_0 : \quad \omega \cdot \nabla I + (\sigma + \kappa)I = \frac{\sigma}{4\pi} \int_{\mathbb{S}^2} I d\omega + \kappa B(T, \nu), \quad (2)$$

where $\kappa(\nu)$ is the absorption coefficient, $\sigma(\nu)$ is the scattering coefficient and $B(\nu, T)$ is the spectral intensity of the black-body radiation given by the Planck's function

$$B(\nu, T) = \frac{2\hbar\nu^3}{c_0^2} (e^{\hbar\nu/kT} - 1)^{-1}. \quad (3)$$

Here \hbar , k and c_0 are Planck's constant, Boltzmann's constant and the speed of radiation propagation in vacuum, respectively. Further physical details can be found in (Mihalas and Mihalas, 1984). In order to minimize the number of parameters, the following non-dimensional variables are introduced

$$\mathbf{x}^* = \frac{\mathbf{x}}{\mathbf{x}_{\text{ref}}}, \quad \sigma^* = \frac{\sigma}{\sigma_{\text{ref}}}, \quad \kappa^* = \frac{\kappa}{\kappa_{\text{ref}}},$$

$$\mathbf{u}^* = \frac{\mathbf{u}}{\mathbf{u}_{\text{ref}}}, \quad T^* = \frac{T}{T_{\text{ref}}}, \quad I^* = \frac{I}{I_{\text{ref}}},$$

where \mathbf{x}_{ref} , σ_{ref} , κ_{ref} , \mathbf{u}_{ref} , T_{ref} and I_{ref} are reference quantities. We also introduce

$$t^* = c\rho(\sigma^* + \kappa^*)\mathbf{x}^* \frac{T^*}{I^*} \quad \text{and} \quad K^* = \frac{I^*}{(\sigma^* + \kappa^*)T^*}.$$

With a diffusion scale, $\varepsilon \in (0, 1]$, defined as

$$\varepsilon = \frac{1}{(\sigma^* + \kappa^*)\mathbf{x}^*},$$

we may write the equations (1)-(2) in dimensionless form as

$$\varepsilon^2 \frac{\partial T}{\partial t} + \varepsilon^2 \mathbf{u} \cdot \nabla T - \varepsilon^2 \nabla \cdot (K \nabla T) = - \int_{\nu_0}^{\infty} \int_{\mathbb{S}^2} \kappa (B(\nu, T) - I) d\omega d\nu, \quad (4)$$

$$\forall \nu > \nu_0 : \quad \varepsilon \omega \cdot \nabla I + (\sigma + \kappa)I = \frac{\sigma}{4\pi} \int_{\mathbb{S}^2} I d\omega + \kappa B(\nu, T), \quad (5)$$

where we have dropped the * superscript for ease of notation. The formulation is completed by specifying appropriate boundary conditions for T and I , as well as an initial condition for T . In our code, these conditions can be easily changed from one type to another in their corresponding subroutines.

3. Fast Multilevel Methods

The numerical method we propose for solving the radiation conduction problem (4)-(5) requires at each time step linear and nonlinear solvers for systems of algebraic equations induced by discretization of time variable t , space variable \mathbf{x} and angle variable ω . Discrete ordinates and Galerkin discretizations have been widely applied to radiative heat transfer in participating media. The methods need single formulation to invoke higher order approximations, integrate easily into existing finite element, finite difference or finite volume codes, guarantee conservation of radiant energy, and are applicable to steady and transient problems, compare (Fiveland, 1991, Lewis and Miller, 1984, Adams and Larsen, 2000). For time discretization of (4) we use the Crank-Nicolson method. Other discretizations can be also straightforwardly included in our algorithm.

One potential drawback of the above discretizations is that the size of the system of equations that needs to be solved grows rapidly as the number of discrete directions increases. Specifically, the size of the discrete systems scales with the number of discrete angles retained in the computation, which increases rapidly with the number of dimensions and with order of discrete ordinates set. Furthermore, since the equations governing the radiation-conduction are coupled, the CPU time needed to solve the fully discrete system can increase rapidly with system size. This poses a serious computational challenge, which requires the development of efficient solvers. The present study aims at this objective, in the context of the radiation-conduction problem given in equations (4)-(5). We implement an efficient multilevel algorithm for accelerating convergence of iterative methods. The method alternates between an iteration that quickly reduces local (high frequency) errors, and the approximate solution on a coarse grid for reducing the global (low frequency) error.

Let us write the equations (4)-(5) in formal way as a fixed point problem for the temperature T only,

$$T = \mathcal{H}(T), \quad (6)$$

with the map $T \rightarrow \mathcal{H}(T)$ is obtained by

$$\mathcal{H}(T) = \mathcal{G}\left(\mathbf{u}, \int_{\nu_0}^{\infty} \kappa \left(4\pi B(\nu, T) - \mathcal{S}(\varphi, B(\nu, T))\right) d\nu\right), \quad (7)$$

where φ denotes the mean intensity

$$\varphi = \int_{\mathbb{S}^2} I d\omega,$$

and $\mathcal{S}(\varphi, q)$ is the solution operator for the radiative transfer problem

$$\forall \nu > \nu_0 : \quad \varepsilon \omega \cdot \nabla I + (\sigma + \kappa)I = \frac{\sigma}{4\pi} \varphi + \kappa q, \quad (8)$$

and $\mathcal{G}(\mathbf{u}, Q)$ is solution operator for the heat conduction problem

$$\varepsilon^2 \frac{\partial T}{\partial t} + \varepsilon^2 \mathbf{u} \cdot \nabla T - \varepsilon^2 \nabla \cdot (K \nabla T) = Q, \quad (9)$$

Note that both problems (8) and (9) can be discretized and solved separately with different discretizations and solvers. Since multilevel methods are widely used, we will briefly recall the main ingredients of the approach, namely (i) the definition of grid levels and (ii) the projection and prolongation procedures.

(i) *Definition of grid levels.* In regular computational domain, the coarsening is made by merging a set of neighboring grid cells to give a single cell on the next coarser grid level. This leads to a hierarchical set of grids. In the current implementation, a coarsening step consists of merging eight cells (two in each direction) with volume areas $\Delta x^l \times \Delta y^l \times \Delta z^l$ each to obtain a child cell with volume area $\Delta x^{l+1} \times \Delta y^{l+1} \times \Delta z^{l+1} = 8\Delta x^l \times \Delta y^l \times \Delta z^l$, the superscripts denoting the respective grid level. Thus, starting from a grid level l , made of $Nx^l \times Ny^l \times Nz^l$ cells, the next grid level contains $Nx^{l+1} \times Ny^{l+1} \times Nz^{l+1} = Nx^l \times Ny^l \times Nz^l / 8$ cells. Clearly, this process can be repeated as long as Nx^l , Ny^l and Nz^l are even numbers. Whenever two or one of the number of cells in a direction is odd, the coarsening automatically switches to a two- or one-dimensional coarsening procedure in which only four or two cells are merged to make a child cell. It is clear that the procedure is optimal when Nx , Ny and Nz are powers of 2. A simple illustration is shown in figure 1.

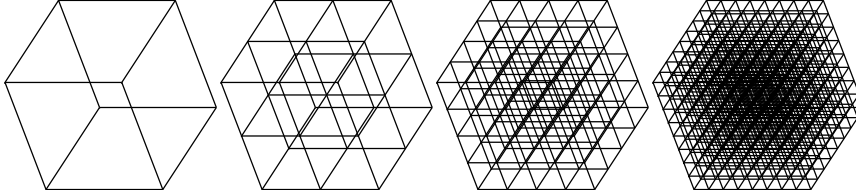


Figure 1. Example of grid coarsening used for the multilevel algorithm.

(ii) *Projection and prolongation procedures.* Let assume a given sequence of nested grids on the computational domain Ω

$$\Omega_1 \subset \Omega_2 \subset \dots \subset \Omega_{L-1} \subset \Omega_L,$$

We use the subscripts l and L to refer to the coarse and fine level respectively. Thus, the problem statement (6) becomes:

Solve on the finest mesh Ω_L the nonlinear system of equations

$$\mathcal{R}_L(T_L) = 0, \quad (10)$$

where \mathcal{R}_L is the residual associated to the fixed point problem (6),

$$R_L(T_L) = T_L - \mathcal{H}_L(T_L).$$

In order to apply multilevel algorithms for the solution operators \mathcal{S} and \mathcal{G} we need the fine-to-coarse grid transfer operator \mathcal{I}_L^l and the coarse-to-fine grid transfer operator \mathcal{I}_l^L . A trivial, efficient and easy

to implement class of operators to perform these steps are, bilinear interpolation for \mathcal{I}_l^L and simple injection for \mathcal{I}_L^l . For more discussions and other different operators we refer to text book (Hackbusch, 1985).

3.1. SOLUTION METHOD FOR RADIATIVE TRANSFER

A fully discretization of the radiative transfer equation (5) is formulated by discretizing the angle and space variables in the equation. The method of discrete ordinates was first introduced and used in (Chandrasekhar, 1950) to solve well many basic problems in the area of radiative transfer. The idea of the discrete ordinates method is very simple indeed: various integral terms in some form of the Boltzmann equation are replaced by numerical quadrature approximations to those terms, and then a resulting set of ordinary differential equations is solved. This corresponds to expanding the integrals on the unit sphere \mathbb{S}^2 in terms of N weighted quadrature rules,

$$\int_{\mathbb{S}^2} I(\nu, \mathbf{x}, \omega) d\omega \simeq \sum_{\ell=1}^N \bar{w}_\ell I(\nu, \mathbf{x}, \omega_\ell), \quad (11)$$

where $\omega_\ell = (\mu_\ell, \eta_\ell, \xi_\ell)^T$, for all $\ell = 1, \dots, N$, with $N = n(n+2)$, and n is the number of direction cosines. Since $\omega_\ell \in \mathbb{S}^2$, we have

$$\mu_\ell^2 + \eta_\ell^2 + \xi_\ell^2 = 1, \quad \text{for all } \ell = 1, 2, \dots, N.$$

We assume n an even number of quadrature points so that the points $(\mu_\ell, \eta_\ell, \xi_\ell)$ are nonzero, symmetric with respect to the x -, y - and z -axis and they are invariant under 90° rotations. Furthermore they satisfy the relation

$$\xi_i^2 = \xi_1^2 + 2 \frac{i-1}{n-2} (1 - 3\xi_1^2),$$

for $i = 1, 2, \dots, \frac{n}{2}$ and $0 < \xi_1 < \frac{1}{3}$.

In (11), \bar{w}_ℓ are the corresponding weights chosen to be positive and satisfy

$$\sum_{\ell=1}^N \bar{w}_\ell = 4\pi, \quad \sum_{\ell=1}^N \bar{w}_\ell \mu_\ell = 0, \quad \sum_{\ell=1}^N \bar{w}_\ell \eta_\ell = 0 \quad \text{and} \quad \sum_{\ell=1}^N \bar{w}_\ell \xi_\ell = 0.$$

Many techniques have been used in the literature to construct accurate discrete S_n sets. Author in (Balsara, 2001) gives a exhaustive survey of several developments and improvement of S_n -discrete ordinate sets. In figure 3 we quote the S_8 from (Lewis and Miller, 1984) widely used in computational radiative transfer.

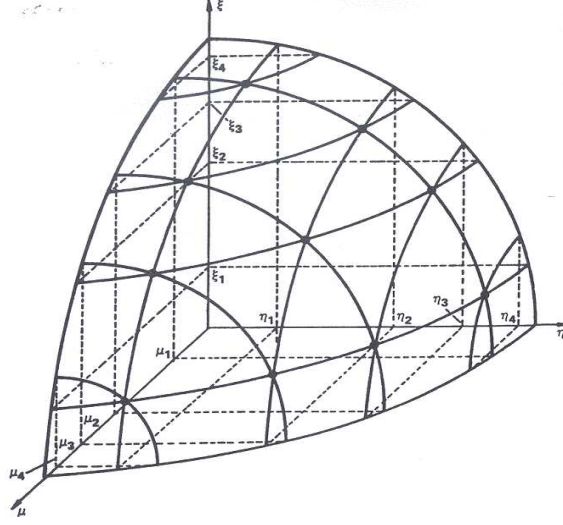


Figure 2. The S_8 set of discrete ordinates as shown in.

Let S_n be a given set of $N = n(n+2)$ discrete directions in \mathbb{S}^2 , then a semi-discrete formulation of (5) reads

$$\forall \nu > \nu_0 : \quad \mu_\ell \frac{\partial I_\ell}{\partial x} + \eta_\ell \frac{\partial I_\ell}{\partial y} + \xi_\ell \frac{\partial I_\ell}{\partial z} + (\sigma + \kappa) I_\ell = \sigma \bar{\phi} + q, \quad (12)$$

with $I_\ell(\nu, x, y, z)$ denotes approximation to $I(\nu, x, y, z, \mu_\ell, \eta_\ell, \xi_\ell)$ and $\bar{\phi}$ is given by

$$\bar{\phi}(\nu, x, y, z) = \frac{1}{4\pi} \sum_{\ell=1}^N \bar{w}_\ell I_\ell(\nu, x, y, z).$$

To discretize the equation (12) in space we define the averaged grid cells

$$x_{i+\frac{1}{2}} = \frac{x_i + x_{i+1}}{2}, \quad y_{j+\frac{1}{2}} = \frac{y_j + y_{j+1}}{2}, \quad z_{k+\frac{1}{2}} = \frac{z_k + z_{k+1}}{2};$$

$$\Delta x_{i+\frac{1}{2}} = x_{i+1} - x_i, \quad \Delta y_{j+\frac{1}{2}} = y_{j+1} - y_j, \quad \Delta z_{k+\frac{1}{2}} = z_{k+1} - z_k,$$

By using the notation f_{ijk} to denote the approximation value of an arbitrary function f at the grid point (x_i, y_j, z_k) , the fully discrete approximation for the equation (8) can be written as

$$\begin{aligned} & \mu_\ell \frac{I_{\ell, i+1jk} - I_{\ell, ijk}}{\Delta x_{i+\frac{1}{2}}} + \eta_\ell \frac{I_{\ell, ij+1k} - I_{\ell, ijk}}{\Delta y_{j+\frac{1}{2}}} + \xi_\ell \frac{I_{\ell, ijk+1} - I_{\ell, ijk}}{\Delta z_{k+\frac{1}{2}}} + \\ & \beta_{i+\frac{1}{2}j+\frac{1}{2}k+\frac{1}{2}} I_{\ell, i+\frac{1}{2}j+\frac{1}{2}k+\frac{1}{2}} = \sigma_{i+\frac{1}{2}j+\frac{1}{2}k+\frac{1}{2}} \bar{\phi}_{i+\frac{1}{2}j+\frac{1}{2}k+\frac{1}{2}} + q_{i+\frac{1}{2}j+\frac{1}{2}k+\frac{1}{2}}, \quad (13) \end{aligned}$$

where $\beta_{i+\frac{1}{2}j+\frac{1}{2}k+\frac{1}{2}} = \sigma_{i+\frac{1}{2}j+\frac{1}{2}k+\frac{1}{2}} + \kappa_{i+\frac{1}{2}j+\frac{1}{2}k+\frac{1}{2}}$ and the cell averages values of I are given by

$$\begin{aligned}
 I_{\ell,i+1jk} &= \frac{1}{\Delta x_{i+\frac{1}{2}}} \int_{y_j}^{y_{j+1}} \int_{z_k}^{z_{k+1}} I_{\ell}(x_i, y, z) dy dz, \\
 I_{\ell,ij+1k} &= \frac{1}{\Delta y_{j+\frac{1}{2}}} \int_{x_i}^{x_{i+1}} \int_{z_k}^{z_{k+1}} I_{\ell}(x, y_j, z) dx dz, \\
 I_{\ell,ijk+1} &= \frac{1}{\Delta z_{k+\frac{1}{2}}} \int_{x_i}^{x_{i+1}} \int_{y_j}^{y_{j+1}} I_{\ell}(x, y, z_k) dx dy, \\
 I_{\ell,ijk} &= \frac{1}{\Delta x_{i+\frac{1}{2}} \Delta y_{j+\frac{1}{2}} \Delta z_{k+\frac{1}{2}}} \int_{x_i}^{x_{i+1}} \int_{y_j}^{y_{j+1}} \int_{z_k}^{z_{k+1}} I_{\ell}(x, y, z) dx dy dz.
 \end{aligned} \tag{14}$$

In this paper we use the Galerkin method to approximate the fluxes in (14). The method consists on centred differences and approximating the function values at the cell centres $f_{i+\frac{1}{2}j+\frac{1}{2}k+\frac{1}{2}}$ by the average of their values at the eight neighboring nodes as shown in figure 3.

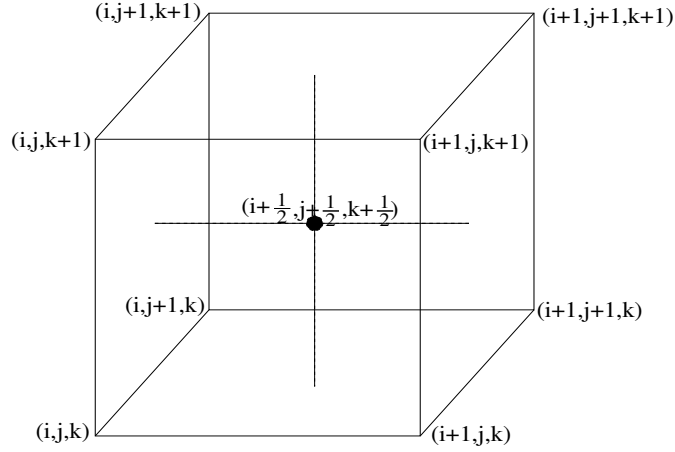


Figure 3. Configuration of the grid cell for space discretization.

Hence the discrete mean intensity $\bar{\phi}_{i+\frac{1}{2}j+\frac{1}{2}k+\frac{1}{2}}$ in (13) is given by

$$\bar{\phi}_{i+\frac{1}{2}j+\frac{1}{2}k+\frac{1}{2}} = \frac{1}{4\pi} \sum_{\ell=1}^N \bar{w}_{\ell} I_{\ell,i+\frac{1}{2}j+\frac{1}{2}k+\frac{1}{2}}.$$

Other discretizations using Legendre polynomial collocation in ordinates and finite element methods in space can be used in the same manner, we refer to (Lewis and Miller, 1984, Brown, 1995, Turek, 1993, Turek, 1995) for details.

By eliminating the spectral intensity from the resulting discretized equations (13), the final linear system to solve for φ on the fine grid Ω_L reads

$$(\mathbf{I} - \mathcal{A}_L)\varphi_L = \mathbf{f}_L, \quad (15)$$

where the Schur matrix \mathcal{A}_L contains the discretized transport and integral operators from (8), \mathbf{f}_L the right hand side and \mathbf{I} is the identity matrix, see (Seaïd and Klar, 2003) for a detailed matrix formulation of (15) in three-dimensional problems. The multilevel method we consider for (15) is a preconditioned Richardson iteration with Atkinson-Brakhage approximate inverse (Kelley, 1995) as preconditioner. Thus,

$$\varphi_L^{(k+1)} = (\mathbf{I} - \mathbf{B}_l^L \mathcal{A}_L)\varphi_L^{(k)} + \mathbf{B}_l^L \mathbf{f}_L, \quad (16)$$

with the Atkinson-Brakhage smoother \mathbf{B}_l^L is given by

$$\mathbf{B}_l^L = \mathbf{I} + \mathcal{A}_l^{-1}(\mathbf{I} - \mathcal{A}_L).$$

Given the finest level $\{L, \mathcal{A}_L, \mathbf{f}_L\}$, the coarsest level $\{l, \mathcal{A}_l, \mathbf{f}_l\}$, the initial guess $\varphi^{(0)}$ and the tolerance τ , the multilevel iteration $\text{NestAB}(m, l, \varphi^{(0)}, \mathbf{f}, \tau)$ for solving (15) is carried out in the following steps:

Algorithm 1: $\text{NestAB}(m, l, \varphi^{(0)}, \mathbf{f}, \tau)$

For $m = l$, $\text{NestAB}(l, l, \varphi_l^{(0)}, \mathbf{f}_l, \tau)$ is the solution obtained by the GMRES algorithm with initial guess $\varphi_l^{(0)}$ and tolerance τ to solve the problem $(\mathbf{I} - \mathcal{A}_l)\varphi_l = \mathbf{f}_l$

For $m = l+1, \dots, L$, $\text{NestAB}(m-1, m, \varphi_m^{(0)}, \mathcal{A}_m, \tau)$ is obtained in the following steps: (we denote by $\text{Gmres}(\mathcal{A}, \mathbf{f}, \varphi^{(0)}, \tau)$ the result of the GMRES algorithm applied to the linear system $(\mathbf{I} - \mathcal{A})\varphi = \mathbf{f}$ with initial guess $\varphi^{(0)}$ and tolerance τ)

do $k = 0, 1, \dots$

a) compute the residual

$$\mathbf{r}^{(k)} = \mathbf{f}_m - (\mathbf{I} - \mathcal{A}_m)\varphi_m^{(k)}$$

b) set

$$\mathbf{u}_{m-1} = \mathcal{I}_m^{m-1}(\mathcal{A}_m \mathbf{r}^{(k)})$$

c) solve on the coarse level

$$\mathbf{v}_{m-1} = \text{Gmres}(\mathcal{A}_{m-1}, \mathbf{u}_{m-1}, \mathbf{v}_{m-1}^{(0)}, \tau_{m-1})$$

d) update the solution

$$\varphi_m^{(k+1)} = \varphi_m^{(k)} + \mathcal{I}_{m-1}^m (\mathcal{A}_{m-1} \mathbf{v}_{m-1}) + \mathcal{A}_m \mathbf{r}^{(k)} + \mathbf{r}^{(k)}$$

e) compute the new residual

$$\mathbf{r}^{(k+1)} = \mathbf{f}_m - (\mathbf{I} - \mathcal{A}_m) \varphi_m^{(k+1)}$$

$$\text{if} \left(\frac{\|\mathbf{r}^{(k+1)}\|_{L^2}}{\|\mathbf{r}^{(0)}\|_{L^2}} \leq \tau \right) \text{ stop}$$

end do

Here $\|\cdot\|_{L^2}$ denotes the discrete L^2 -norm. The tolerance parameters $\{\tau_m\}$ for stopping the iterations in the GMRES method, can be considered either fixed or adaptively chosen as in (Kelley, 1995).

3.2. SOLUTION METHOD FOR HEAT CONDUCTION

The obtained solution operator \mathcal{S} from **Algorithm 1** is used to formulate the right hand side in the heat conduction stage (9). In order to discretize the solution operator \mathcal{G} we assume the same sequence of nested grids and the same space discretization as those used in the previous subsection for the operator \mathcal{S} . Moreover, by using the Crank-Nicolson time integration scheme the equation (9) can be transformed into a steady heat equation where the time stepsize Δt is incorporated into the diffusion coefficient and the right hand term.

Newton's method applied to (10) results in the following iteration

$$T_L^{(k+1)} = T_L^{(k)} - \mathcal{R}'_L(T_L^{(k)})^{-1} \mathcal{R}_L(T_L^{(k)}), \quad (17)$$

where \mathcal{R}'_L is the system Jacobian approximated by a difference quotient of the form

$$\mathcal{R}'_L(T_L^{(k)})_{\mathbf{w}} \approx \frac{\mathcal{R}_L(T_L^{(k)} + \delta \mathbf{w}) - \mathcal{R}_L(T_L^{(k)})}{\delta}. \quad (18)$$

If a GMRES method (Saad and Schultz, 1986) is used to compute the Newton direction then, at each time step the following algorithm has to be called in the time loop:

Algorithm 2: $NGmres(\mathcal{H}_L, T^{(0)}, \tau)$

Given \mathcal{H}_L , tolerance τ and initial guess $T^{(0)}$ chosen to be the solution at the previous time step, the Newton-Gmres algorithm for solving (10) uses the following steps: (we denote by $\text{Gmres}(\mathcal{A}, \mathbf{f}, \varphi^{(0)}, \tau)$ the result of Gmres algorithm applied to linear system $\mathcal{A}\varphi = \mathbf{f}$ with initial guess $\varphi^{(0)}$ and tolerance τ)

do $k = 0, 1, \dots$

a) compute the residual

$$\mathcal{R}_L^{(k)} = T_L^{(k)} - \mathcal{H}_L(T_L^{(k)})$$

b) solve using Gmres,

$$\mathbf{d}_L^{(k)} = \text{Gmres}(\mathcal{R}'_L(T_L^{(k)}), -\mathcal{R}_L(T_L^{(k)}), \mathbf{d}^{(0)}, \tau^{(k)})$$

c) update the solution

$$T_L^{(k+1)} = T_L^{(k)} + \xi \mathbf{d}_L^{(k)}$$

if $(\|T_L^{(k+1)}\|_{L^2} \leq \tau)$ stop

end do

The Newton step ξ , the tolerance $\tau^{(k)}$ to stop the inner iterations in Gmres, and the difference increment δ in (18) are selected according to backtracking linesearch, Eisenstat-Walker and Hardwired techniques as discussed in details by (Kelly, 1995).

The m th-level iteration $\text{NestNG}(m, l, T^{(0)}, \tau)$ in nested Newton-Gmres algorithm to solve (10) can be implemented as follows:

Algorithm 3: $\text{NestNG}(m, l, T^{(0)}, \tau)$

For $m = l$, $\text{Nestng}(l, l, T_l^{(0)}, \tau)$ is the solution obtained by the Ngmres algorithm with input parameters \mathcal{H}_l , $T_l^{(0)}$ and τ

For $m = l+1, \dots, L$, $\text{NestNG}(m-1, m, T_m^{(0)}, \tau)$ is obtained by:

a) initialize

$$T_m = \mathcal{I}_{m-1}^m(T_{m-1})$$

b) set

$$\tau_m = \frac{\|\mathcal{H}_m(T_m)\|_{L^2}}{10}$$

c) solve $NGmres(\mathcal{H}_m, T_m^{(0)}, \tau_m)$
 end do

The step *b*) in **Algorithm 3** ensures that the incoming residual will be reduced by a factor of 10 at each level (Banoczy and Kelley, 1998).

4. Numerical Results

We have selected two test examples to check the performance of our multilevel methods. The algorithms formulated in this paper have been tested on a PC with AMD-K6 200 processor running Fortran codes under Linux 2.2. In all these methods the iterations are terminated when the relative residuals satisfy

$$\frac{\|\mathbf{r}^{(m)}\|_{L^2}}{\|\mathbf{r}^{(0)}\|_{L^2}} \leq 10^{-6}.$$

We would like to point out that an extensive comparative study of the present algorithms to other numerical methods from computational radiative transfer has recently been reported in (Seaïd et al., 2004) for the two-dimensional radiative heat transfer in both grey and non-grey media. In this section we shall show results only for grey computations ($B(T, \nu) = B(T) = kT^4$ with k is the Boltzmann's constant).

4.1. EXAMPLE 1

Our first test example is the radiative transfer equation in unit cube with fixed temperature distribution

$$\mu \frac{\partial I}{\partial x} + \eta \frac{\partial I}{\partial y} + \xi \frac{\partial I}{\partial z} + (\sigma + \kappa)I = \frac{\sigma}{4\pi} \int_{\mathbb{S}^2} I(\omega', x, y, z) d\omega' + \kappa B(T(x, y, z)).$$

The temperature is chosen as a linearly increasing function from 1800 K to 2400 K as

$$T(x, y, z) = 400x + 200z + 1800. \quad (19)$$

The wall boundaries are considered ingoing Planckians with fixed temperature given by (19). The main idea behind considering this test example is the comparison of efficiency of the solution operator \mathcal{S} to the well established solvers from computational radiative transfer.

First, in table I we summarize the run times for different mesh hierarchies for two-level NestAB (NestAB2) algorithm. Here, we set

Table I. Run times (in seconds) at different mesh hierarchies for the two-level NestAB2 algorithm.

Gridpoints	CPU time
$16 \times 16 \times 16$	0.18
$32 \times 32 \times 32$	3.78
$64 \times 64 \times 64$	18.63
$128 \times 128 \times 128$	81.37

$\kappa = 0.1 \text{ m}^{-1}$, $\sigma = 10 \text{ m}^{-1}$ and we used the S_8 set of discrete ordinates for discretization of the unit sphere S^2 .

Next, we compare the convergence rates for the NestAB2 algorithm with other iterative solvers widely used in the literature to approximate solution to radiative transfer. Hence, figure 4 illustrates the convergence rates for the NestAB2, the Source Iteration (SI), Diffusion Synthetic Acceleration (DSA), and GMRES algorithms using different scattering and absorbing media. The associated CPU times to these algorithms are listed in table II. We also included in this table the CPU time for the Atkinson-Brakhage (AB) algorithm. In all these results the S_8 set for discrete ordinates and a fine mesh of $64 \times 64 \times 64$ gridpoints are used in the computations.

Table II. CPU times (in seconds) for SI, GMRES, DSA, AB and NestAB2 algorithms on fine mesh of $64 \times 64 \times 64$ gridpoints.

	$\kappa = 0.1, \sigma = 1$	$\kappa = 0.1, \sigma = 10$	$\kappa = 0.1, \sigma = 100$
SI	13.8	52.8	1214.4
GMRES	11.4	23.4	191.14
DSA	277.8	391.8	459.0
AB	10.8	20.4	121.8
NestAB2	10.8	18.6	76.2

From the above listed results one observes, for large scattering coefficients, that the SI method is unacceptably slow to converge. The convergence rate is improved significantly by GMRES, and it is improved even more by DSA method but at the cost of extra work and storage. The most effective method for solving this example, however, is the multilevel NestAB2 algorithm.

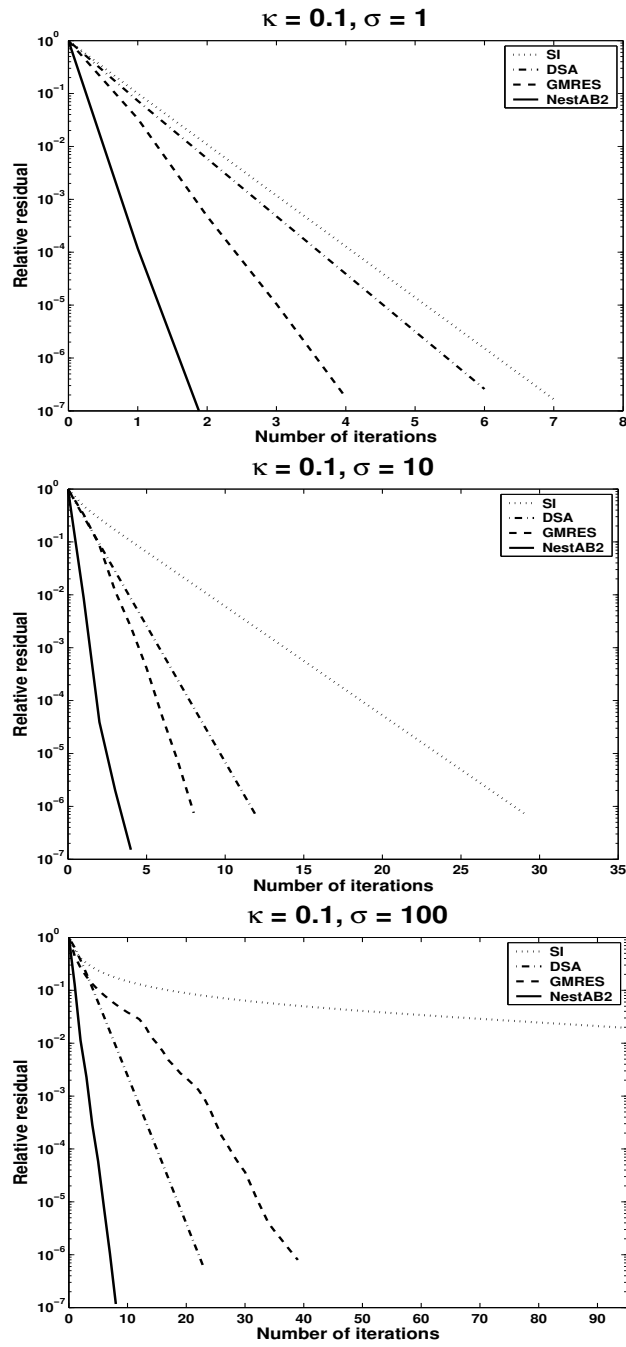


Figure 4. Convergence rates for radiative transfer equation with fixed temperature using different absorption and scattering coefficients.

4.2. EXAMPLE 2

In this test example we consider a radiative heat conduction problem in cooling process. The problem statement is given by the dimensionless equations (4)-(5) where a geometry $\Omega = [0, 3] \times [0, 1] \times [0, 1]$ initially at temperature $T = 1800$ evolves in cooling process at surrounded temperature $T = 500$. Figure 5 shows the temperature distribution at $t = 0.1$ on a part of the domain Ω covered with $180 \times 60 \times 60$ gridpoints.

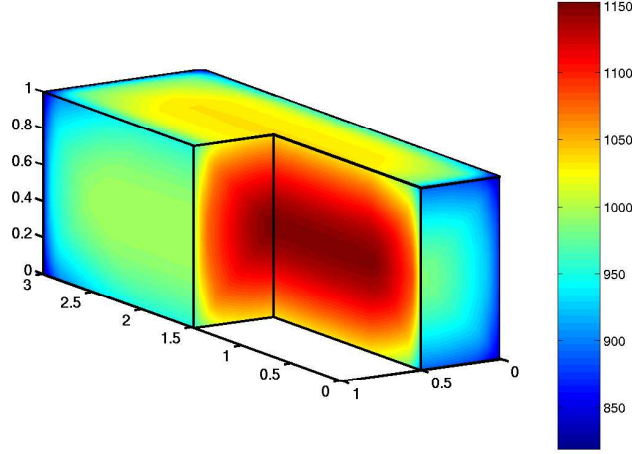


Figure 5. The dimensionless temperature at $t = 0.1$ on a part of the computational domain using $\kappa = 1$, $\sigma = 1$, $\varepsilon = 1$ and $180 \times 60 \times 60$ gridpoints.

Table III. CPU time (in minutes) for NG, NestNG2, NestNG3, NestNAB2 and NestNAB3 algorithms on a fine mesh of $180 \times 60 \times 60$ gridpoints.

	$\varepsilon = 1$	$\varepsilon = 0.1$	$\varepsilon = 0.01$
NG	11.93	16.94	21.51
NestNG2	4.77	6.34	7.23
NestNG3	5.01	6.07	7.39
NestNAB2	3.52	4.01	5.21
NestNAB3	3.89	4.94	7.01

In table III, we compare the run times for the different methods for this radiative heat conduction problem. We compare Newton Gmres (NGmres), two-level nested Newton Gmres (NestNG2), three-level

nested Newton Gmres (NestNG3), two-level Newton Atkinson-Brakhage (NestNAB2), three-level nested Newton Atkinson-Brakhage (NestAB3).

The results reported in table III are obtained on a fine mesh with $180 \times 60 \times 60$ gridpoints using three different radiation regimes corresponding to $\varepsilon = 1$, $\varepsilon = 0.1$ and $\varepsilon = 0.01$. The time stepsize is fixed to $\Delta t = 10^{-3}$ and results are computed for a time $t = 0.1$. The difference among the CPU times with different radiative regimes increases as the scaling parameter ε decreases. It is clear that in all cases, the multilevel algorithm gives the most efficient results than other solvers even in the diffusive regime ($\varepsilon = 0.01$).

Our next concern is to test the influence of spectral discretization on the efficiency of multilevel methods. To this end, we run the NestNG2 algorithm using different S_n sets of discrete ordinates. In table IV, comparison of run times for S_2 , S_4 , S_6 and S_8 sets are given for the same parameters as those used in figure 5. As can be seen from the table, the use of higher order discretizations for the unit sphere leads to considerable increase in the computational work in NestNG2 algorithm.

Table IV. CPU time (in minutes) in NestNG2 algorithm for different S_n sets of discrete ordinates.

	$\varepsilon = 1$	$\varepsilon = 0.1$
S_2 -solution	0.24	0.28
S_4 -solution	0.97	1.09
S_6 -solution	2.19	2.49
S_8 -solution	3.52	4.01

In order to show the effect of using higher order discrete-ordinates approximation on accuracy, cross sections at $y = 0.5$ and $z = 0.5$ of the temperature from figure 5 have been plotted in figure 6 for the considered S_n sets. As can be seen from the figure, higher order S_n discretization leads to considerable improvement in the accuracy of the predicted temperature. Note that, increasing the order of approximation from S_6 to S_8 does not lead for significant improvement in the predicted accuracy.

5. Concluding Remarks

A robust multilevel method for solving the three-dimensional radiation and heat conduction in high temperature computations has been devel-

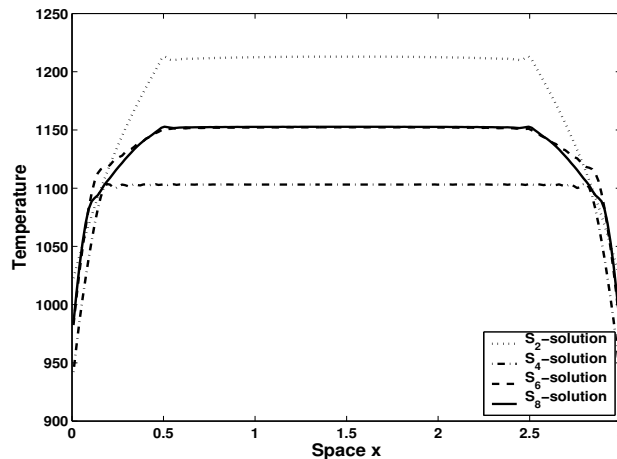


Figure 6. A cross section of the dimensionless temperature at $y = 0.5$ and $z = 0.5$ for different S_n sets of discrete ordinates.

oped and tested. The method combines the discrete ordinates method with a Galerkin discretization in space, while an implicit time integration procedure is used for the heat conduction. The fully discretization leads to a linear and nonlinear system of equations to be solved at each time step for the mean intensity and the temperature, respectively. In our algorithm, the Atkinson-Brakhage approximate inverse and Newton-Gmres method are used as smoothers on the coarse level for solving the linear and nonlinear equations, respectively.

Validation of the algorithm has been carried out using two test examples. The algorithm exhibited high efficiency and good stability behavior. Furthermore, numerical illustrations in the present work indicate the possibility of employing the same tools to attack a wide variety of radiative heat conduction problems arising in high temperature chambers, industrial furnaces and other engineering fields. At present, we are trying to adapt this method to more difficult problems, such as those used in gas turbine combustion chambers. The equations in this model are strongly nonlinear and involve hydrodynamics and chemistry effects. We believe that for these problems, the multilevel algorithms might be very effective since they reduce the number of iterations needed for convergence and they are relatively inexpensive to implement.

It is worthwhile to remark that the presented multilevel algorithms are designed in such a way they can easily be integrated in an existing CFD code for hydrodynamical flows. Furthermore, the discretization of time, angle and space can be easily changed according to the problem

under consideration. Finally, we want to point out that, the parallel implementation of the methods presented in this paper is straightforward and only requires interprocessor communication to complete the matrix-vector and vector-vector products required at each iteration.

References

- Adams, M. and E. Larsen: 2000, 'Fast Iterative Methods for Deterministic Particle Transport Computations'. *Preprint*.
- Balsara, D.: 2001, 'Fast and Accurate Discrete Ordinate Methods for Multidimensional Radiative Transfer. Part I, Basics Methods'. *JQSRT* **69**, 671–707.
- Banoczi, J. and C. Kelley: 1998, 'A Fast Multilevel Algorithm for the Solution of Nonlinear Systems of Conductive-Radiative Heat Transfer Equation'. *SIAM J. Sci. Comput.* **19**, 266–279.
- Briggs, W., V. Henson, and S. McCormick: 1999, *A Multigrid Tutorial*. SIAM, second edition.
- Brown, P.: 1995, 'A Linear Algebraic Development of Diffusion Synthetic Acceleration for Three-Dimensional Transport Equations'. *SIAM. J. Numer. Anal* **32**, 179–214.
- Chandrasekhar, S.: 1950, *Radiative Transfer*. Oxford Univ. Press, London.
- Fiveland, W.: 1991, 'The Selection of Discrete Ordinate Quadrature Sets for Anisotropic Scattering'. *ASME HTD. Fundam. Radiat. Heat Transfer* **160**, 89–96.
- Frank, M., M. Seaïd, J. Janicka, K. A., R. Pinnau, and G. Thömmes: 2004, 'A Comparison of Approximate Models for Radiation in Gas Turbines'. *Int. J. Progress in CFD* **3**, 191–197.
- Hackbusch, W.: 1985, *Multi-Grid Methods and Applications*. Springer Series in Computational Mathematics, vol 4 Springer-Verlag, New York,.
- Jamaluddin, A. and P. Smith: 1988, 'Predicting Radiative Transfer in Axisymmetric Cylindrical Enclosures using the Discrete Ordinates Method'. *Combustion Science and Technology* **62**, 173–186.
- Kelley, C.: 1995, 'Multilevel Source Iteration Accelerators for the Linear Transport Equation in Slab Geometry'. *Transp. Theory and Stat. Phy.* **24**, 679–707.
- Kelly, C.: 1995, *Iterative Methods for Linear and Nonlinear Equations*. SIAM. Philadelphia.
- Lewis, E. and W. Miller: 1984, *Computational Methods of Neutron Transport*. John Wiley & Sons, New York.
- Liu, F., H. Becker, and Y. Bindar: 1998, 'A Comparative Study of Radiative Heat Transfer Modelling in Gas-Fired Furnaces using the Simple Grey gas and the Weighted-sum-of grey-gases Models'. *International Journal Heat and Mass Transfer* **41**, 3357–3371.
- McCormick, S.: 1989, *Multilevel Adaptive Methods for Partial Differential Equations*. SIAM.
- Mihalas, D. and B. Mihalas: 1984, *Foundations of Radiation Hydrodynamics*. Oxford Univ. Press, New York.
- Saad, Y. and M. Schultz: 1986, 'GMRES: A Generalized Minimal Residual Algorithm for Solving Nonsymmetric Linear Systems'. *SIAM. J. Sci. Statist. Comput.* **7**, 856–869.

- Seaïd, M., M. Frank, A. Klar, R. Pinnau, and G. Thömmes: 2004, 'Efficient Numerical Methods for Radiation in Gas Turbines'. *J. Comp. Applied Math* **170**, 217–239.
- Seaïd, M. and A. Klar: 2003, 'Efficient Preconditioning of Linear Systems Arising from the Discretization of Radiative Transfer Equation'. *Lecture Notes in Computational Science and Engineering* **35**, 211–236.
- Selcuk, N.: 1988, 'Evaluation for Radiative Transfer in Rectangular Furnaces'. *International Journal Heat and Mass Transfer* **31**, 1477–1482.
- Selcuk, N. and N. Kayakol: 1997, 'Evaluation of Discrete Ordinates Method for Radiative Transfer in Rectangular Furnaces'. *International Journal Heat and Mass Transfer* **40**, 213–222.
- Steward, F. and P. Cannon: 1971, 'The Calculation of Radiative Heat Flux in a Cylindrical Furnace using the Monte Carlo Method'. *International Journal Heat and Mass Transfer* **14**, 245–262.
- Turek, S.: 1993, 'An Efficient Solution Technique for the Radiative Transfer Equation'. *IMPACT, Comput. Sci. Eng.* **5**, 201–214.
- Turek, S.: 1995, 'A Generalized Mean Intensity Approach for the Numerical Solution of the Radiative Transfer Equation'. *Computing* **54**, 27–38.